Effect of Ethanol Addition on the Drainage Time of Aqueous/Ethanol NFC Suspensions and on Barrier and Mechanical Properties of the Produced Films

VLD Costa[1,2*] and RMS Simões[1,2]

[1]Research unit of Fiber Materials and Environmental Technologies (FibEnTech-UBI), Universidade da Beira Interior, Covilhã, Portugal

[2]Department of Chemistry, University of Beira Interior, Covilha, Portugal

*Corresponding author: Vera Lúcia Dias da Costa, Research Unit of Fiber Materials and Environmental Technologies (FibEn-Tech-UBI) Universidade da Beira Interior, Rua Marquês d'Avila e Bolama, 6200-001 Covilhã, Portugal, Tel: +351275319739, E-mail: vera. costa@ubi.pt

Citation: VLD Costa (2022) Effect of Ethanol Addition on the Drainage Time of Aqueous/Ethanol NFC Suspensions and on Barrier and Mechanical Properties of the Produced Films. J Mater sci Appl 6: 1-13

Abstract

NFC aqueous/ethanol suspensions with a solid content 0.3 wt.% were produced from a TEMPO-oxidized bleached kraft eucalypt pulp, with ethanol content varying from o to 75 wt.%. Films were manufactured from these suspensions through vacuum filtration at a constant absolute pressure, and the draining progression was monitored by measuring the collected filtrate. The NFC filtration cakes were adhered to metallic discs and kept under pressure applied to the edges while they dried either in standard conditions of temperature and humidity or in an oven at 70ºC for 4 hours. The resulting films were tested for mechanical and optical performance and water vapor barrier properties. Results show that filtrating time decreases drastically with the increase of ethanol content, from about 2 hours to 2 minutes for 0 and 75 wt.% ethanol suspensions, respectively. The films' porosity generally increased with the increase of ethanol content. The mechanical performance of standard dried films was not affected by increasing ethanol content, despite the global porosity increase from 18.8% to 31.3%. On the other hand, the tensile index drastically increased for oven-dried films up to 124 and 90.2 N m g^{-1} for 0 and 75 wt.% ethanol suspensions, respectively, despite significant increase in elongation and scattering coefficient. Water vapor transmission rate increased up to 207.48 g m^{-2} day^{-1} for films produced from 75 wt.% ethanol suspensions.

Keywords: Nano Fibrillated Cellulose; Ethanol; Films Production; Drainage Time; Mechanical Performance; Water Vapor Barrier.

Introduction

Nanotechnology is a field that researches nanomaterials, which are materials with structural units on a nanometer scale in at least one direction. These materials have enhanced and desirable chemical and physical properties, that can be tailored and harvested according to several diverse applications, such as light-harvesting and bioelectricity [1]; scaffolds for bone tissue engineering [2, 3] and composite thermally insulating materials [4].

Nanocellulosic materials have strong self-association tendency and an inherent predisposition to form films upon drying through strong interactions within the numerous surface hydroxyl groups. These films have unique physical properties such as high strength and translucency or even fully transparency, depending on the overall dimensions of the individual fibrils [5].

The inherent strength of crystalline cellulose combined with the strong interfibrillar interaction can be harvested in order to manufacture mechanically robust NFC-based films with excellent oxygen barrier properties in dry conditions and susceptible to functionalization [6,7].

NFC films usually have a good mechanical resistance, with tensile strength and Young's modulus typically varying within 100–200 MPa and 5–10 GPa, respectively, although large variation in mechanical behavior can be expected due to numerous reasons such as the chemical composition of the NFC raw material and chemical/ mechanical pretreatments, which directly influence the fibril size and size distribution as well as the amount of interfibrillar contacts within the formed films [5].

The resistance to solvents, even to water, is another useful property of dried films made from NFC aqueous suspensions: while soaking normal dried pulp sheets in water causes weakening and structure disintegration into individual fibers due to their strong interaction with water through hydrogen bonding, NFC films, on the other hand, remain resilient after extended contact with solvents such as ethanol, acetone, and toluene or even water. Hornification due to additional hydrogen bonding in the amorphous regions of cellulose and consequent irreversible fibril agglomeration has been suggested as the reason behind this observed solvent resistance [8-10].

Several authors have reported the manufacture of NFC based films through filtration of NFC suspensions, followed by hot-pressing the NFC filtering cake under high loads in order to avoid wrinkling and considerably reduce the drying time, besides improving the mechanical properties due to the densification of the structure [10 - 12] but, depending on the material used in the filtration and pressing processes, the films can end up not being entirely smooth, or with some level of irregularities on their surface [10].

Furthermore, the most acknowledged drawback of the majority of the reported approaches concerning pure NFC films formation is the extremely slow dewatering of NFC aqueous suspensions, making the process extremely time-consuming, usually requiring several hours to a few days and with complicated manipulations [10].

Many authors have reported filtrating times that go anywhere from 45 minutes [11] to 3-4 hours [13] using fine pore size filter media (0.65 μm and 0.1 μm), depending on the filtrated volume, operating conditions, intended grammage and on the morphology of the fibrils, which can also play an important role in the draining progression [14].

In an effort to fasten the filtrating process, some authors have tried increasing the pore size of the filtrating medium [10,14], but it came with a drawback. Österberg et al. have reported a fast method for producing NFC films through pressurized filtration using an open mesh fabric with a 10 μm pore size at 2.5 bar pressure [10]. The filtration process took less than an hour, but at the expenses of losing 40% of the material through the pores during the process, for every produced film. Lower drainage time (up to 3 minutes) and with 94% fibril retention was reported by Varanasi and Batchelor, applying vacuum of 25 MPa through a 125 μm woven copper wire mesh filter medium [12].

Another reported technique for filtration aid is the addition of high molecular weight cationic polyacrylamide [15]. The authors have analyzed the flocculation and water drainability of an MFC gel as a function of the polyelectrolyte dosage, charge density and molecular weight, and reported a drainage time as low as to 9.5 minutes, giving rise to highly porous films, suggesting a retention of a more open colloidal structure of the material upon drying. Despite the fast film formation process, the resulting material was a cellulose-based composite rather

than a purely nanocellulosic film, since both cellulosic fibrils and added polyelectrolyte were combined in on single structure.

While solvent exchange to a non-aqueous media of previously drained or casted NFC aqueous suspensions is extensively performed either to prevent structural changes during subsequent surface modification, tailor the porosity of the film or to fasten the drying process [6, 16 -19], to the best of our knowledge, no studies have been undertaken concerning the formation of neat NFC films from ethanol/aqueous suspensions.

The present work aims to study the effect of NFC aqueous/ethanol suspensions composition on the drainage time and specific resistance of the NFC cake during NFC films formation through vacuum filtration and on barrier/mechanical properties of the resulting films.

Materials and Methods

A commercial Totally Chlorine Free (TCF) never dried bleached kraft eucalypt pulp (average limiting viscosity was 570 mL/g) was utilized as a source of native cellulose fibers. Ethanol 99% (Sigma-Aldrich, USA) was used without further purification.

NFC suspensions production

The NFC suspension was produced in an analogous way to a previously reported work [20]. In resume, a commercial never dried bleached kraft eucalypt pulp was submitted to 2 successive homogenization steps at 500 and 850 bar, using a GEA Niro Soavi high pressure homogenizer (Panther NS3006L; GEA, Parma, Italy), and was afterwards submitted to 2,2,6,6-tetramethylpiperidine-1-oxyl radical (TEMPO) mediated oxidation.

Morphological characterization of the fibrils

In order to morphologically characterize the cellulose fibrils in the obtained NFC suspension, a drop of 0.01 wt.% NFC suspension was allowed to air dry overnight at room temperature on a scanning electron microscope (SEM) sample holder.

The samples were previously gold sputtered by cathodic spraying (Quorum Q150R ES; Quorum Technologies, East Sussex, UK) and microscopic observations were performed using SEM (Hitachi S-2700; Hitachi, Tokyo, Japan) operated at 20 kV.

For the transmission electron microscope (TEM) imaging, drops of 0.001 wt% NFC suspension were deposited on carbon-coated electron microscopic grids and negatively stained with 2 wt% uranyl acetate. The grids were air-dried and analyzed with a Hitachi HT-7700 TEM (Hitachi, Tokyo, Japan) with an acceleration voltage of 80 kV.

Cellulose degree of polymerization

The NFC limiting viscosity (η) was determined according to the ISO 5351 (2012) standard, with a cupriethylenediamine (CED) solution as a solvent and using a capillary viscometer. The degree of polymerization (DP) was calculated using the literature' equations [6].

Total acidic groups content

The total acidic groups content in the produced NFC was determined through a conductivity titration method, based on the standard SCAN-CM 65:02, as described in a previous paper [20].

Production of films from NFC aqueous/ethanol suspensions

The previously produced NFC suspension was diluted to a solid content of 0.3 wt.%, using the required amounts of water and ethanol, and homogenized (Ultra-Turrax T-25 Digital Homogenizer, Ika Labortechnik, Staufen, Germany) for 2 minutes at 6000 rpm. The resulting suspension was subjected to a mild ultrasound bath (S30H, Elmasonic, Singen, Germany) for 5 minutes to release the air bubbles.

Simple NFC films with a diameter of 8.5 cm and a target grammage of 50 g m^{-2} were prepared by vacuum filtration in a filtrating funnel, using a 0.65 μm pore size nitrocellulose membrane (Millipore, Bedford, Mass., USA) as filtration medium, attached to a filter paper for added support. Vacuum filtration was carried out at a constant absolute pressure of 0.2 bar, using a vacuum pump. The draining progression was monitored by collecting the filtrate and weighing it along the filtration time. The filtrations were considered to be over whenever the drainage stopped.

The NFC wet filtration cake and filtrating membrane were placed between blotting papers, followed by pressing for 5 minutes at 2.19 x 10^5 N m^{-2}. Then, a metallic disc was thorough-

ly placed on top of the film, and the whole set was once again pressed for an additional 10 seconds at the same pressure, just enough for the NFC film to adhere to the metallic disc. The filtrating membrane was removed at this stage. Finally, the NFC films were dried, between perforated metallic rings under pressure applied to the edge of the films in order to prevent them from shrinking. The films were dried either overnight in a standard atmosphere for conditioning (23 ºC and 50 % of relative humidity), or in an oven at 70ºC for 4 hours. The oven dried films were conditioned in standard conditions overnight before testing.

Characterization of films produced from NFC aqueous/ethanol suspensions

The basis weight of the films was calculated according to ISO 536:2012 and their thickness was measured with a micrometer (Adamel & Lhomargy, M120 series, New York, USA). The arithmetic average of four measurements was used.
The apparent density of the films was determined from the basis weight and thickness.
The corresponding porosity of the films was estimated according to the equation (1).

$$Porosity\ (\%) = 100 \times 1 - \left(\frac{\rho_{film}}{\rho_{cellulose}}\right) \qquad (1)$$

Where ρ_{film} is the apparent density of the film, g/cm³ and $\rho_{cellulose}$ is the density of crystalline cellulose, which is assumed to be 1.6 g/cm³.

The tensile properties of the produced films were tested according to ISO 187:1990. The tensile strength, elongation at break and Young's modulus were determined using an universal tensile testing equipment (Thwing-Albert Instrument Co., EJA series, Philadelphia, USA) with a load cell of 100 N and a constant rate of elongation (20 mm.min⁻¹), according to ISO 1924-2:2008. The distance between grips was 50 mm. To avoid slippage at the sample holders, small pieces of paper tape were attached to the edges of the samples.

Static bending stiffness was performed by a bending tester (Lorentzen & Weltre, Sweeden) at an angle of 25 degrees and a 50 mm distance, according to an adaptation made from ISO 5628:2012. For all tests, at least four representative films have been tested and the arithmetic average values are presented. The optical properties of the films (brightness (ISO 2470-1:2009) and transparency) were determined through spectrophotometry (Technidyne Corp., Color Touch® 2, France).

Water vapor barrier properties

The water vapor transmission rate (WVTR) was determined for the produced films according to Tappi 448 om-09. Home customed containers were used, ensuring constant water vapor partial pressures in both sides of the films throughout the essays. The interior of the containers had a given amount of anhydrous granular calcium chloride that ensured zero water vapor partial pressure inside the recipients. The other side of the films was in contact with the standard conditions of temperature and humidity of the laboratory. The amount of water vapor that diffused through the films was accounted by the mass increase of the whole set. The whole sets were periodically weighted for as long as 144 hours and the mass gain was used to determine the WVTR (g (m² day)⁻¹) of each sample, according to the equation (2).

$$WVTR = \frac{S}{A} \qquad (2)$$

Where S corresponds to the slope of a liner regression that best fits the plot of weight gain *vs* testing time (g days⁻¹) and A is the area of the films (m²).

Statistical analysis

The experimental data were subjected to statistical analysis using SPSS 28 software (SPSS Inc., Chicago, USA) and were examined using analysis of variance (ANOVA). Tukey's test was used to verify the significant differences among the values at $p < 0.05$.

Results and Discussion

Morphological characterization of the fibrils

The morphology of the fibrils was investigated through observations with SEM and TEM in order to give an overview on the present micro- and nanoscale elements. Figure 1 depicts the morphological characteristics of the produced NFC.
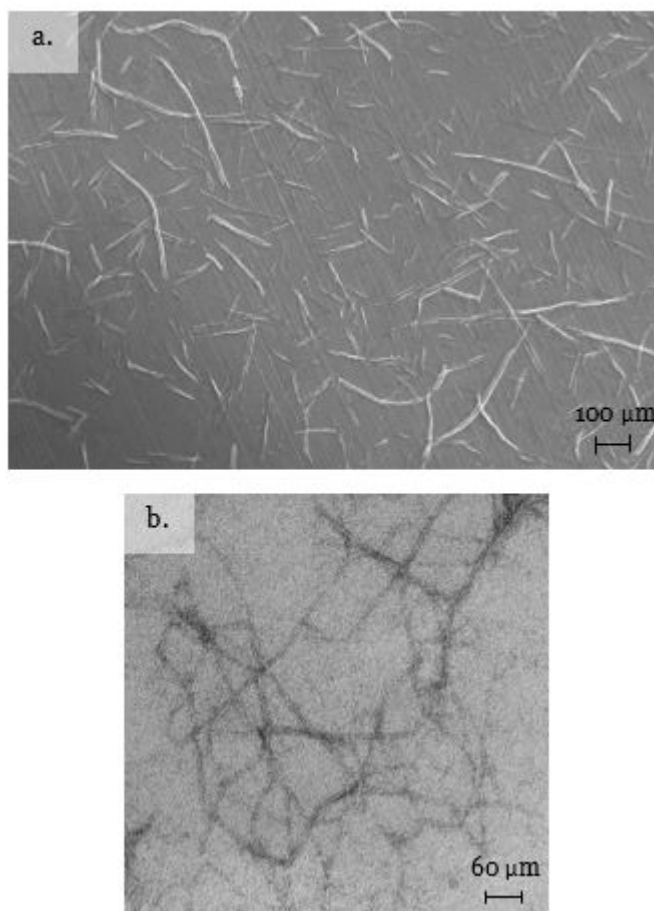
Figure 1: NFC fibrils imaged through SEM (a) and TEM (b)

As Figure 1 shows, the pulp has been disintegrated into nanofibrils (Figure 1, b), although many microscale elements are also observable (Figure 1, a).

Physico-chemical characterization of the fibrils

The TEMPO-oxidized fibrils had a determined limiting viscosity of 154 mL/g, corresponding to a calculated average DP of 367, which are by far lower than those of the starting material (limiting viscosity of 570 ml/g, corresponding to a DP of 1429). The resulting average carboxyl groups content was 997 μmol/g. These results are in good agreement with what has been reported in the literature for similar pretreatments using TEMPO/NaBr/NaClO oxidation systems [21 - 23].

Draining evaluation

The drainage progression throughout filtration of the aqueous/ethanol NFC suspensions is depicted in Figure 2.

At the end of the filtration process, the total recovered filtrate was not the same in every essay due to some evapora-tion, but Figure 2 makes clear that the filtrating rate increases drastically with the increase of ethanol content in the suspension. While an aqueous NFC suspension (o wt.% ethanol) took around 180 minutes, increasing the ethanol content to 50, 60 and 75 wt.% fastened the filtration process to around 120, 18 and 2 minutes, respectively, using a 0.65 μm pore size nitrocellulose membrane as a filtration medium.

To further characterize the NFC suspension filtration process, the data was analyzed based on the Hagen-Poiseuille's equation (equation 3), taking in account that the transmembrane pressure (ΔP) is constant (0.8×10^5 N m^{-2}).

$$\frac{At}{V} = \frac{\mu \, \alpha \, \rho_0}{2 \, \Delta P} \times \frac{V}{A} + \frac{\mu \, R_M}{\Delta P} \qquad (3)$$

Where A is the filtrating membrane area (m^2); t is the filtrating time (s); V is the filtrate volume (m^3); μ is the filtrate viscosity (Pa s); α is the cake specific resistance; R_M is the membrane specific resistance; ρ_0 is the weight of cake per unit volume of filtrate (kg m^{-3}); ΔP is the transmembrane pressure (N m^{-2}).

Under these circumstances, the representation of At/V as function of V/A should give a linear plot, where intercept of the linear regression is related to the R_M and the slope is related to the α, if the cake is incompressible.

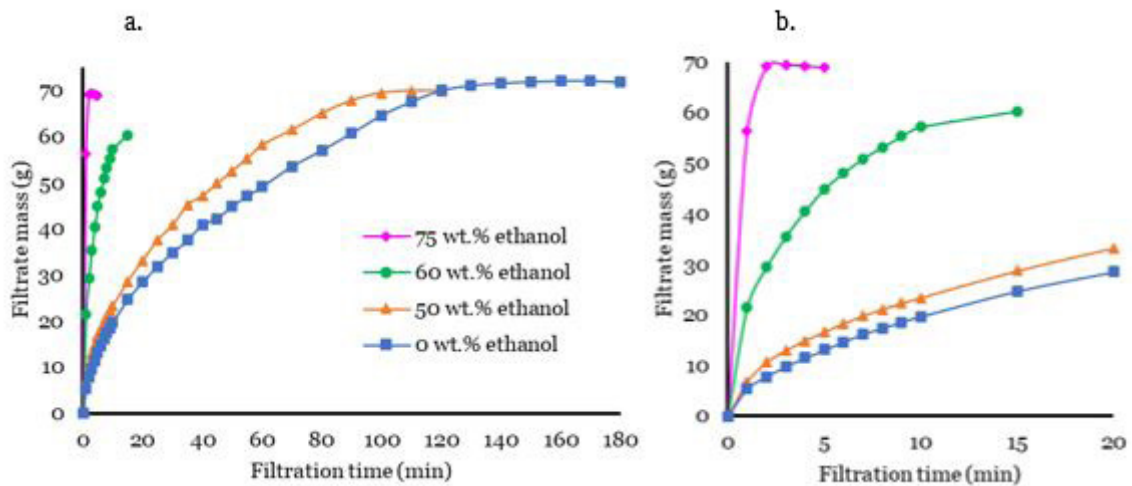Figure 3 represents this profile for the NFC aqueous suspension (0 wt.% ethanol).

Figure 2: Monitorization of drainage during the manufacture of films from NFC suspensions with different ethanol contents: a.) total filtration time; b.) zoom in of the first 20 minutes of filtration
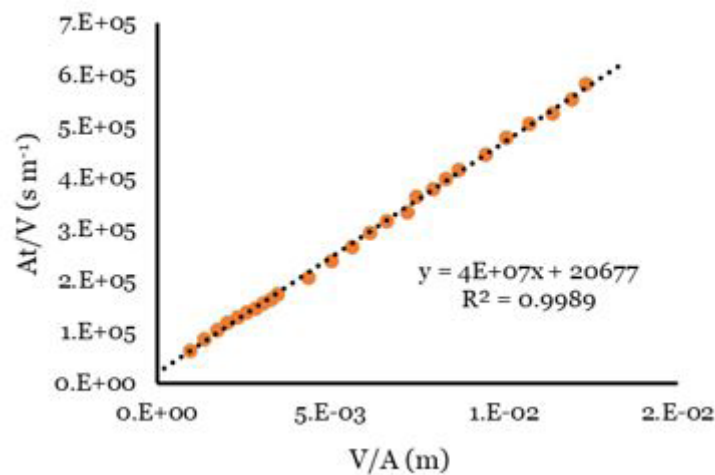

Figure 3: Linear regression of At/V as function of V/A in an NFC aqueous suspension filtration process

As we can see in Figure 3, the experimental values have an excellent linear fitting, with an R^2 over 0.99, confirming that this cake is incompressible and thus it is possible to estimate both α and R_M. The same data treatment was performed on the subsequent essays with increasing ethanol content; the fittings were also good, but the specific membrane resistance appears negative, which indicates some deviation from the model. The calculated α and R_M are presented in Table 1, taking into account the change of the viscosity of the medium, which increases somewhat with ethanol addition.

As expected from the drainage profiles in Figure 2, the NFC cake specific resistance decreases drastically with the addition of ethanol to the aqueous NFC suspension. Theoretically, the cake specific filtration resistance depends on the cake porosity and specific surface area of the particles. As we will see later in the paper, the porosity of the dry film increases significantly from 18.8% for 0 and 50 wt.% ethanol to 25.5% and 31.3%, respectively for 60 and 75wt.% ethanol (Table 2). The wet thickness of the cake could not be measured due to the fragile nature of the film, but the dry thickness suggests that the porosity of the wet

cake increases with the ethanol content of the aqueous suspension. Considering that ethanol induces some fibrils aggregation, we can speculate that the specific surface area of the particles was also reduced.

Table 1: Calculated cake specific resistance (α) membrane specific resistance (R_M) and for filtration of NFC suspensions with different ethanol contents

Ethanol content (wt.%)	α	R_M
0	2.13×10^{15}	1.65×10^{12}
50	6.95×10^{14}	-3.07×10^{10}
60	1.04×10^{14}	-2.29×10^{11}
75	3.82×10^{13}	-4.79×10^{11}

Mechanical and optical characterization of the films

In order to study the effect of the suspensions' composition and drying conditions on the mechanical and optical properties, the produced films were either air dried in standard temperature and relative humidity conditions (22ºC and 50% RH) or in an oven at 70ºC for 4 hours. Oven dried films were conditioned in standard conditions for 24 hours before testing. Table 2 shows the results.

As it was aforementioned, the porosity of the films dried in standard conditions generally increases with the increase of ethanol content. While the high surface tension of water (about 70 dyne/cm) promotes pore collapse between fibrils and hydrogen bond area development upon drying, the ethanol with its much lower surface tension (about 20 dyne/cm) and lower boiling point is less effective in the interfibrillar pores collapse, leading to structures with higher global porosities. In addition, when exposed to less polar media, the cellulosic fibrils' network undergoes partly irreversible reorganization, like aggregation, tending to the energetically most favorable state and thus more porous structures arise from this process [9, 24]. On the other hand, while NFC films made from 0 wt.% ethanol suspensions exhibited the same porosity either when dried in standard conditions or in the oven, oven dried films made from 50, 60 and 75 wt.% ethanol NFC suspensions increased the porosity by over 60% concerning their dry standard conditions counterparts. The oven drying process decreases even more the surface tension of ethanol and provides energy for fast ethanol evaporation, further increasing the global film porosity.

Regarding the mechanical properties of the films dried in standard conditions, the results put in evidence that the tensile index and Young's modulus of the NFC films (Table 2) are not substantially affected by the increase of ethanol content in the suspension from which they were produced, which is a very positive result taking in account that the film formation time decreases from close to 2 hours to around 2 minutes. What is even more interesting is the drastic increase of the tensile index when the films were dried in an oven during 4 hours at 70ºC; for the 0 wt.% ethanol/aqueous suspension, the increase in tensile index reaches 73% (71.6 to 124 N m g^{-1}), despite the significant increase in elongation (from 1.7% to 6.1%). For the ethanol/water suspensions, the relative tensile index increase is in the range of 30-40%, despite both increase in elongation and porosity. For the films made from 75 wt.% ethanol/aqueous suspensions, the higher performance of the oven dried films, regarding the standard dry films, persisted; the tensile index increased about 31%, despite the much higher elongation and scattering coefficient (2.1 *vs* 6.3% and 6.49 *vs* 15.05 cm²/g, respectively). In resume, the oven dried films produced from 75 wt.% ethanol/water NFC suspension exhibited higher mechanical performance (92.2 N.m/g *vs* 71.6 N.m/g) than the dry standard films produced from 100 wt.% water NFC suspension. This performance is obtained, despite the much higher global porosity of the film (50% *vs* 18.8%) and higher elongation 6.3% *vs* 1.7%), which highlights the potential of both ethanol addition to the NFC suspension and the oven drying process.

Usually, the increase in mechanical resistance takes place at the expenses of a loss in elongation and an increase in contact between structural elements (evidenced in a decrease in the scattering coefficient). In the present study this was not the

case; both the elongation and the scattering coefficient increase considerably, whereas the tensile index also increases drastically, which puts in evidence the role of curing temperature on the film's properties.

Österberg *et al.* performed hot-pressing of films produced through filtration of NFC aqueous suspensions, at about 100 °C and 1800 Pa, varying the pressing time between 0.5 and 2 hours. The authors reported an increase from 121 MPa to 180 MPa (corresponding to an increase in tensile index from 149.6 N.m/g to 219.3 N.m/g), which puts in evidence the positive role of the temperature on the mechanical properties of the NFC films. Elongation, however, decreased substantially when the pressing time increased from o.5 to 2h, from 7.9 to 5.1% [10]

Regarding the optical properties, Table 2 shows that films produced from purely aqueous NFC suspensions (0 wt.% ethanol) reached a transparency of over 83 % for standard dried films and over 71 % for oven dried films, which is in the same transparency range of the results reported by Huang *et al.* [25]. These authors produced nanopapers through filtration of

a TEMPO oxidized NFC aqueous suspension using a 0.65 μm pore size nitrocellulose ester filter membrane, followed by hot pressing at 105°C, and obtained NFC films with transparencies of around 90% [25]. Furthermore, Fukuzumi *et al.* reported transmittances at 600 nm of about 90% and 78% for NFC films prepared through vacuum filtration from softwood cellulose and from hardwood cellulose, respectively [26].

In the present research, the transparency of the films dried under standard conditions remains constant until 60% of ethanol content and decreases substantially for the 75 wt.% ethanol NFC suspension. The transparency decreases considerably for the oven dry process relative to the standard dry one. These results generally agree with the scattering coefficient since films with higher scattering coefficients are likely to appear less transparent. Increasing scattering coefficient and brightness generally coincided with a decrease in apparent density and an increase in the porosity of the films, which is in good agreement with Zhu *et al.* who reported that light transmittance and scattering in transparent nanopapaers do not only depend on the fibrils size but also on the packing density of the structure [27].

Table 2: Mechanical and optical characterization of NFC films produced from NFC suspensions with different ethanol compositions

Suspensions' ethanol content (wt.%)	Drying conditions*	Grammage (g m^{-2})	Apparent density (g cm^{-3})	Porosity (%)	Tensile index (N m g^{-1})	Elongation (%)	Young's modulus (GPa)	Bending stiffness (mN)	ISO Brightness (%)	ISO Opacity (%)	Transparency (%)	Scattering coefficient (cm^2 g^{-1})
0	Standard	47.5± 2.6^a	1.3± 0.05^a	18.8± 3.0^a	71.6± 8.3^a	1.7± 0.3^a	6.4 ± 0.4^a	72.5± 0.2^a	36.42± 1.09	26.91± 2.51	83.81± 1.61	0.04±0.07
	Oven	46.9± 1.3^a	1.3± 0.06^a	18.8± 3.6^a	124.0± 15.4^b	6.1± 2.4^b	5.9± 1.4^d	76.3± 0.1^e	36.01± 1.03	47.03± 1.93	71.96± 1.31	2.00±0.02
50	Standard	51.8± 0.5^b	1.3± 0.05^a	18.8± 3.3^a	75.4± 11.8^a	1.6± 0.5^a	6.9± 0.6^a	85.0± 1.3^b	38.19± 0.48	26.49± 1.14	83.43± 0.78	0.14±0.01
	Oven	50.3± 0.6^b	1.1± 0.01^b	31.3± 0.9^c	99.7± 13.2^c	6.5± 1.4^b	4.5± 0.8^e	88.8± 0.1^f	41.67± 0.57	39.70± 1.19	75.22± 0.65	3.41±0.03
60	Standard	50.3± 1.0^b	1.2± 0.01^b	25.0± 0.8^b	62.2± 7.1^b	1.5± 0.4^a	6.2± 0.5^b	91.3± 0.2^c	40.15± 0.60	27.30± 1.32	82.86± 0.92	2.91±0.21
	Oven	50.3± 0.8^b	0.9± 0.01^b	43.8± 0.5^d	87.3± 6.2^d	6.8± 0.6^b	3.3± 0.1^f	97.5± 0.2^g	69.31± 0.65	71.20± 2.03	47.52± 0.10	15.74±0.14
75	Standard	51.5± 1.7^b	1.1± 0.05^b	31.3± 3.0^c	70.4± 11.3^a	2.1± 0.6^a	5.4± 0.2^c	82.5± 0.3^d	43.16± 3.36	36.29± 4.13	72.92± 3.19	6.49±0.99
	Oven	51.0± 0.1^b	0.8± 0.01^b	50.0± 0.7^e	92.2± 7.1^e	6.3± 1.1^b	3.2± 0.1^f	110.0± 0.3^h	58.01± 2.21	69.52± 3.74	48.83± 2.45	15.05±0.85

* Drying conditions: Standard is air dried overnight at 22°C and 50% RH; Oven is oven dried at 70°C for 4 hours

Means at the same column with different superscript letters are significantly different (p < 0.05)

Figure 4 shows a side-by-side comparison of films produced from 75wt.% ethanol and 0 wt.% ethanol NFC suspensions, dried under standard conditions. The higher opacity of the former film is in accordance with its higher light scattering coefficient (6.49 cm^2/g *vs* 0.04 cm^2/g) and higher global porosity. The combination of drying in the oven and film production from ethanol/water suspension provided the opportunity to manipulate film transparency, preserving the mechanical performance.

The bending stiffness of the films, in general, increases as the global porosity increase, due to the increase in film thickness

Water vapor transmission through the films

Regarding the water vapor transmission though the films, the WVTR of films made from solely aqueous NFC suspensions are on the same range as those reported by other authors [28, 29].

As it is evidenced in Figure 5 and Table 3, the WVTR is not substantially affected when the ethanol content of the NFC suspension increases up to 60 wt.%, even though the film's porosity increases from 18.8 to 25% for 0 or 50 and 60 wt.% ethanol, respectively. However, a notorious increase from 134.83 to 207.48 g m^{-2} day^{-1} takes place by increasing the ethanol content to 75%, accordingly accompanied by an increase in the porosity from 25.0 to 31.3%.

The oven drying process caused a further increase of over 40% in the WVTR of the films made from a 75 wt.% ethanol suspension (207.48 to 291.19 g m^{-2} day^{-1}), against an increase of around 60% on the porosity (31.3 to 50%). Interestingly, the oven dried NFC films made from 0 wt.% ethanol suspensions increased the WVTR by 19% (137.82 to 163.83 g m^{-2} day^{-1}) despite the porosity remained unaltered.

In resume, filtrating a 75 wt.% ethanol/aqueous NFC suspension and oven drying at 70ºC for 4 hours, decreased the film formation time from around 2 hours to 2 minutes, providing a film with tensile properties higher than those exhibited by an air-dried film produced from an aqueous NFC suspension. Furthermore, the films produced from this method exhibited higher WVTR and porosity.
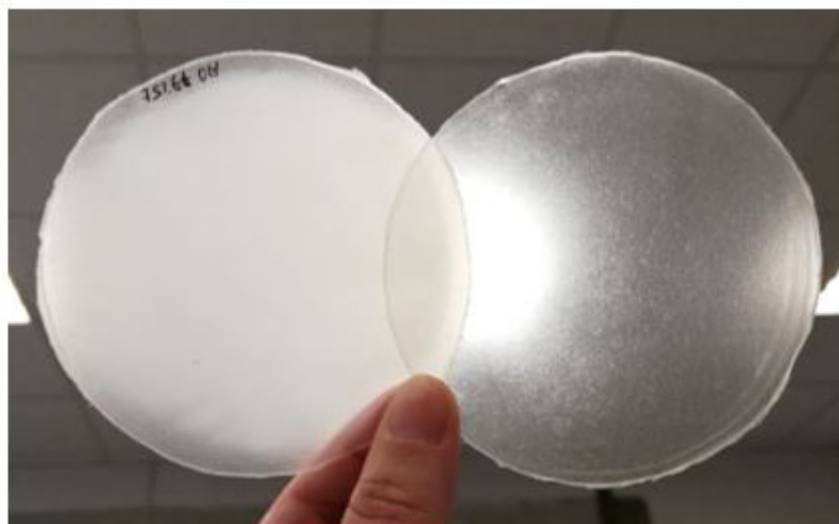

Figure 4: Films produced from a 75wt.% ethanol NFC suspension (left) and from a purely aqueous NFC suspension (right) dried under standard conditions

Table 3: Calculated water vapor transfer rate for films produced from different ethanol content NFC suspensions and different drying conditions

Ethanol content (wt.%)	Drying conditions	WVTR (g m^{-2} day^{-1})	Porosity (%)
0	Standard	137.82	18.8
50		137.52	18.8
60		134.83	25.0
75		207.48	31.3
0	Oven	163.83	18.8
75		291.19	50.0
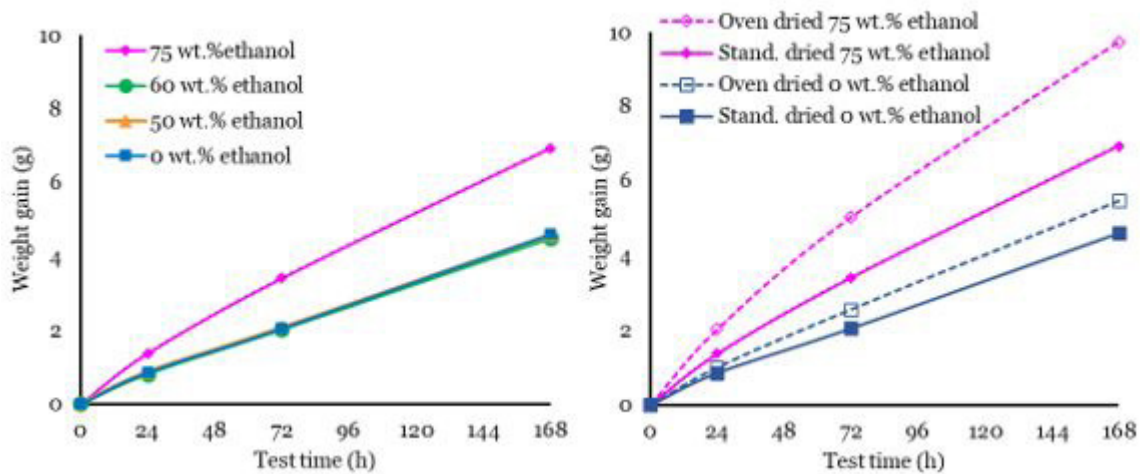
Figure 5: Transferred water vapor as a function of test time for NFC films produced from different ethanol content NFC suspensions

Conclusions

The main specific conclusions of the work are the following:

• The addition of ethanol to the NFC aqueous suspension to attain a 75 wt.% ethanol content enabled to decrease the filtration time from about 2 hours to about 2 minutes. Using a constant transmembrane pressure of 0.8x 10^5 N/m^2, it was possible to estimate the NFC cake specific resistance. This value decreased from 2.1 x 10^{15} m/kg to 3.8 x 10^{13} m/kg with the ethanol addition (75 wt%. ethanol/aqueous NFC suspension).

• The tensile index and Young's modulus of the standard dried NFC films were not, in general, substantially affected by the increase of ethanol content in the NFC suspensions.

• Oven drying the films (70ºC, 4 hours) enabled to drastically increase the film's tensile index, regarding the standard dried ones. These results were obtained with films with higher global poros-

ity and surprisingly with much higher elongation.

• The porosity of the produced films generally increased with the increase of ethanol content. Oven drying the films made from 50 to 75 wt.% ethanol NFC suspensions resulted in an increase in porosity of over 60%.

• WVTR was not substantially affected when the ethanol content of the NFC suspension increased up to 60 wt.%, but there was a notorious increase from 134.83 to 207.48 g m^{-2} day^{-1} for the films made from 75 wt.% ethanol NFC suspensions. The oven drying process of these films caused a further increase of over 40% in the WVTR.

• The combination of both film drying in oven and film production from ethanol/water suspension provided the opportunity to manipulate film transparency and water vapor transmission rate, preserving the mechanical performance of the films.

In resume, with this study we propose a relatively fast and simple method to produce neat NFC films with potentially desirable mechanical and barrier properties for membrane applications where mechanical strength, toughness, low density, controlled permeability and porosity and high surface area are important, such as fuel cells, liquid purification and filtering, tissue engineering, protein immobilization and separation, and protective clothing.

Acknowledgements

References

1. Mouhib M, Antonucci A, Reggente M, Amirjani A, Gillen AJ, et al. (2019) Enhancing bioelectricity generation in microbial fuel cells and biophotovoltaics using nanomaterials. Nano Res 12: 2184-99.

2. Sadeghpour S, Amirjani A, Hafezi M, Zamanian A (2014) Fabrication of a novel nanostructured calcium zirconium silicate scaffolds prepared by a freeze-casting method for bone tissue engineering. Ceramics Int 40: 16107-14.

3. Amirjani A, Hafezi M, Zamanian A, Yasaee M, Abu Osman N (2016) Synthesis of nano-structured sphene and mechanical properties optimization of its scaffold via response surface methodology. J Advanced Materials and Processing 4: 56-62.

4. Guo W, Wang X, Zhang P, Liu J, Song L, et al. (2018) Nano-fibrillated cellulose-hydroxyapatite based composite foams with excellent fire resistance. Carbohydrate Polymers 195: 71-8.

5. Tammelin T, Vartiainen J (2014) Nanocellulose Films and Barriers. In: Handbook of Green Material. World Scientific Publishing Co. Pte. Ltd: 213-29.

6. Henriksson M, Berglund LA, Isaksson P, Lindström T, Nishino T (2008) Cellulose Nanopaper Structures of High Toughness. Biomacromolecules 9: 1579-85.

7. Lavoine N, Desloges I, Dufresne A, Bras J (2012) Microfibrillated cellulose - Its barrier properties and applications in cellulosic materials: A review. Carbohydrate Polymers 90: 735-64.

8. Hult EL, Larsson PT, Iversen T (2001) Cellulose fibril aggregation — an inherent property of kraft pulps. Polymer 42: 3309-14.

9. Johansson LS, Tammelin T, Campbell JM, Setälä H, Österberg M (2011) Experimental evidence on medium driven cellulose surface adaptation demonstrated using nanofibrillated cellulose. Soft Matter, 7: 10917.

10. Österberg M, Vartiainen J, Lucenius J, Hippi U, Seppälä J, et al. (2013) A Fast Method to Produce Strong NFC Films as a Platform for Barrier and Functional Materials. ACS Applied Materials & Interfaces 5: 4640-7.

11. Sehaqui H, Liu A, Zhou Q, Berglund LA (2010) Fast Preparation Procedure for Large, Flat Cellulose and Cellulose/Inorganic Nanopaper Structures. Biomacromolecules 11: 2195-8.

12. Varanasi S, Batchelor WJ (2013) Rapid preparation of cellulose nanofibre sheet. Cellulose 20: 211-5.

13. Nogi M, Iwamoto S, Nakagaito AN, Yano H (2009) Optically transparent nanofiber paper. Advanced Materials 21: 1595-8.

14. Zhang L, Batchelor W, Varanasi S, Tsuzuki T, Wan X (2012) Effect of cellulose nanofiber dimensions on sheet forming through filtration. Cellulose 19: 561-74.

15. Raj P, Varanasi S, Batchelor W, Garnier G (2015) Effect of cationic polyacrylamide on the processing and properties of nanocellulose films. J Colloid and Interface Sci 447: 113-9.

16. Sehaqui H, Zhou Q, Ikkala O, Berglund LA (2011) Strong and Tough Cellulose Nanopaper with High Specific Surface Area and Porosity. Biomacromolecules 12: 3638-44.

17. Sim K, Ryu J, Youn HJ (2015) Structural characteristics of nanofibrillated cellulose mats: Effect of preparation conditions. Fibers and Polymers 16: 294-301.

18. Toivonen MS, Kurki-Suonio S, Schacher FH, Hietala S, Rojas OJ, et al. (2015) Water-Resistant, Transparent Hybrid Nanopaper by Physical Cross-Linking with Chitosan. Biomacromolecules, 16: 1062-71.

19. Solala I, Bordes R, Larsson A (2017) Water vapor mass transport across nanofibrillated cellulose films: effect of surface hydrophobization. Cellulose 25: 347-56.

20. Costa VL, Costa AP, Simões RM (2019) Nanofibrillated Cellulose Rheology: Effects of Morphology, Ethanol/Acetone Addition, and High NaCl Concentration. BioResources 14: 7636-54.

21. Besbes I, Alila S, Boufi S (2011) Nanofibrillated cellulose from TEMPO-oxidized eucalyptus fibres: Effect of the carboxyl content. Carbohydrate Polymers 84: 975-83.

22. Isogai A, Saito T, Fukuzumi H (2011) TEMPO-oxidized

cellulose nanofibers. Nanoscale 3: 71–85.

23.   Shinoda R, Saito T, Okita Y, Isogai A (2012) Relationship between Length and Degree of Polymerization of TEMPO-Oxidized Cellulose Nanofibrils. Biomacromolecules 13: 842-9.

24.   Moon RJ, Martini A, Nairn J, Simonsen J, Youngblood J (2011) Cellulose nanomaterials review: structure, properties and nanocomposites. Chemical Society Reviews 40: 3941.

25.   Huang J, Zhu H, Chen Y, Preston C, Rohrbach K, et al. (2013) Highly Transparent and Flexible Nanopaper Transistors. ACS Nano 7: 2106-13.

26.   Fukuzumi H, Saito T, Iwata T, Kumamoto Y, Isogai A (2008) Transparent and High Gas Barrier Films of Cellulose Nanofibers Prepared by TEMPO-Mediated Oxidation. Biomacromolecules 10: 162-5.

27.   Zhu H, Parvinian S, Preston C, Vaaland O, Ruan Z, et al. (2013) Transparent nanopaper with tailored optical properties. Nanoscale 5: 3787.

28.   Bedane AH, Eić M, Farmahini-Farahani M, Xiao H (2015) Water vapor transport properties of regenerated cellulose and nanofibrillated cellulose films. J Membrane Sci 493: 46-57.

29.   Souza G, Belgacem MN, Gandini A, Carvalho AJF (2021) Low permeable hydrophobic nanofibrilated cellulose films modified by dipping and heating processing technique. Cellulose 28: 1617-32.